Cyclic Softening of the Sn-3.8Ag-0.7Cu Lead-Free Solder Alloy with Equiaxed Grain Structure

QIU-LIAN ZENG,[1] ZHONG-GUANG WANG,[1] AI-PING XIAN,[1] and J.K. SHANG[2]

1.—Shenyang National Laboratory for Materials Science, Institute of Metal Research, Chinese Academy of Sciences, 110016 Shenyang, China. 2.— Department of Materials Science and Engineering, University of Illinois at Urbana–Champaign, Urbana, IL 61801. E-mail: jkshang@uiuc.edu

Low-cycle fatigue behavior of the Sn-Ag-Cu ternary-eutectic alloy was investigated under a fully reversed loading condition. The solder alloy exhibited cyclic softening early in the fatigue life and continued to soften as the number of fatigue cycles increased. Following cyclic loading, numerous microcracks were found in the microstructure. Most of the microcracks were located along the grain boundaries in the areas with finer grains. The areal density of the microcracks increased with both strain amplitude and cycle number. By combining percolation theory with microcracking analysis, the cycle-dependent softening behavior was shown to result from accumulation of microcrack density with fatigue cycles.

Key words: Lead-free solder, low-cycle fatigue, cyclic softening, Sn-3.8Ag-0.7Cu alloy

INTRODUCTION

The ternary Sn-Ag-Cu eutectic alloy is widely considered a leading Pb-free candidate alloy for replacement of Sn-Pb solder alloys in microelectronic packaging because of its attractive mechanical and physical properties.[1–5] As a replacement for the Pb-bearing alloys, the primary function of the Pb-free solder alloy in electronic packages is to provide the necessary interconnection between different parts of the device. In both design and testing of solder interconnections, one of the major concerns to the integrity of the solder interconnect is potential fatigue failures that may result from thermal or mechanical cycling of electronic packages.[6,7]

The fatigue analysis of Pb-bearing solder interconnects is largely based on the low-cycle fatigue behavior of the solder alloy.[6] To support this analysis, a great amount of work has been conducted over the years on fatigue behavior of Pb-bearing solder alloys.[6] While some of the general observations apply to Pb-free solder alloys, significant differences in fatigue mechanisms and properties may result from distinct microstructures of the eutectic Sn-Ag-Cu and Sn-Pb alloys. Recently, Kanchanomai et al.[8] and Kariya and Otsuka[9] investigated the mechanical fatigue of the Sn-Ag-Cu bulk solder alloys and found that the Coffin–Manson equation had to be modified to account for the strong effect of the fracture ductility on the fatigue life of the alloys.

In this study, low-cycle fatigue tests were conducted on the ternary-eutectic alloy with an equiaxed grain structure. The objective of this study was to determine how low-cycle fatigue behavior might be related to micromechanisms of fatigue damage in the eutectic Sn-Ag-Cu alloy. Through microscopic examinations of the fatigued specimens, the dominant fatigue damage mechanism prior to macrocrack development was found to be microcracking. During cyclic loading, microcracks tended to initiate mostly along grain boundaries at the very early stage of the fatigue life. The number and density of the microcracks increased with the number of fatigue cycles so that the specimen was populated with microcracks over nearly the entire fatigue life. The progressive development of the microcracks over the fatigue life resulted in a strong cycle-dependent cyclic-softening behavior. The presence of microcracks over most of the fatigue life raised the question whether deformation-based fatigue analysis without any consideration to those

(Received December 18, 2003; accepted March 25, 2004)

microcracks could be simply extended to the ternary-eutectic Sn-Ag-Cu alloy.

EXPERIMENTAL PROCEDURE

Ingots of the Sn-3.8Ag-0.7Cu solder alloy were prepared by melting high-purity (>99.99) tin, silver, and copper in vacuum at 800°C for 30 min. After furnace cooling, the alloy was remelted at 250°C and cast into a steel mold with a cavity 200 mm × 72 mm × 7 mm. Subsequently, the castings were aged for 3 months at room temperature to stabilize the microstructure. The as-cast microstructure was composed of equiaxed tin-rich grains and needles or nodules of the Ag_3Sn phase, as shown in Fig. 1a. Image analysis indicated that the average grain size was about 50 μm. On the polycrystalline Sn matrix, the Ag_3Sn phase was randomly distributed, with some Ag_3Sn needles running across a single grain and others lying along the grain boundaries (Fig. 1a and b). The length of the Ag_3Sn needle ranged from a couple of microns to about 100 μm. In some areas, Ag_3Sn nodules formed small dendrites.

Low-cycle fatigue tests were conducted on plate specimens with a gauge length of 8 mm and a rectangular cross section of 4 mm × 5 mm. The specimens were cut from the plate casting by electrical discharge machining, ground by sand paper, polished to 0.5-μm diamond finish before fatigue testing. Fatigue tests were performed on a servohydraulic fatigue machine with a 1-kN load capacity. A triangular waveform was used for the fatigue tests. Fully reversed cyclic tests were carried out under the total strain control. The first cycle always started in tension. The tests were conducted at a range of the total strain amplitudes from 0.2% to 1%. In all tests, the strain rate was held constant at 10^{-3} sec^{-1}. During the test, stress-strain response of the specimen was recorded for every cycle by a computer data-acquisition system. On select specimens, fatigue tests were interrupted, and the specimens removed for examination under scanning electron microscopy (SEM).

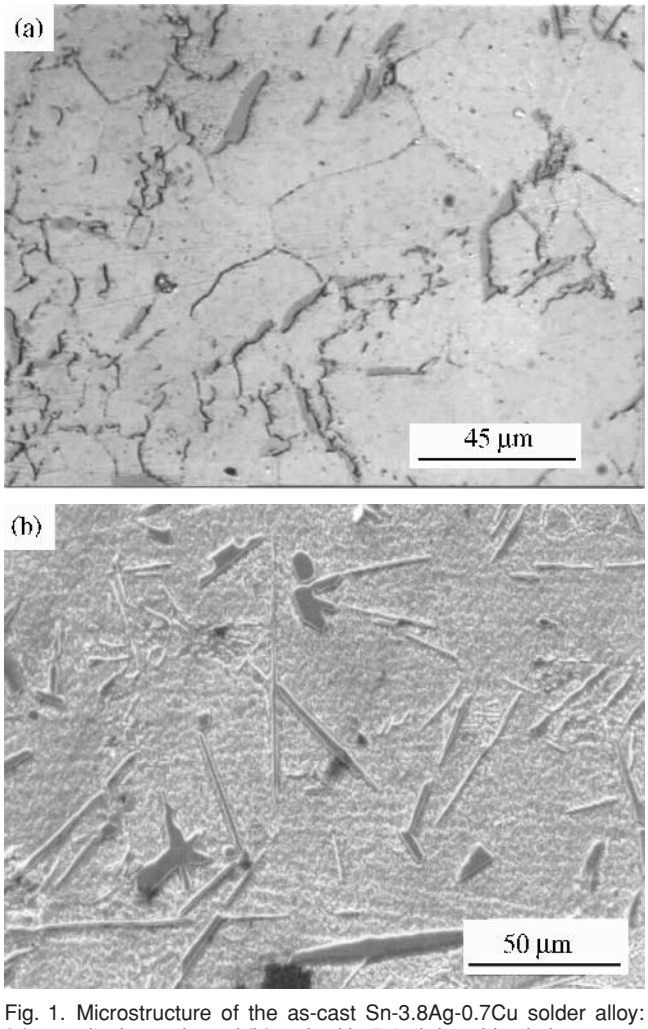

Fig. 1. Microstructure of the as-cast Sn-3.8Ag-0.7Cu solder alloy: (a) unetched sample and (b) etched in 5% nitric acid solution.

RESULTS

Cycle-Dependent Softening

The cyclic response of the Sn-3.8Ag-0.7Cu solder alloy is shown in Fig. 2 by the variation of the stress amplitude with the number of fatigue cycles at three different strain amplitudes under a constant strain rate of 10^{-3} sec^{-1}. The data show that the stress amplitude decreased with the number of fatigue cycles, indicating a cycle-dependent softening behavior. Experiments conducted at additional strain amplitudes of 0.2%, 0.6%, 1.0%, and 1.2% showed similar cycle-dependent softening behavior. With increasing strain amplitudes, cyclic softening was accelerated so that the fatigue life of the specimen was shortened from over 10,000 cycles at a strain amplitude of 0.2% to less than 500 cycles at a strain amplitude of 1.2%.

In most metals, such as aluminum alloys and steels, cycle-dependent softening or hardening behavior, especially at low strain amplitudes, is typically limited to the first few fatigue cycles and cycle-dependent behavior is followed by a steady-state response

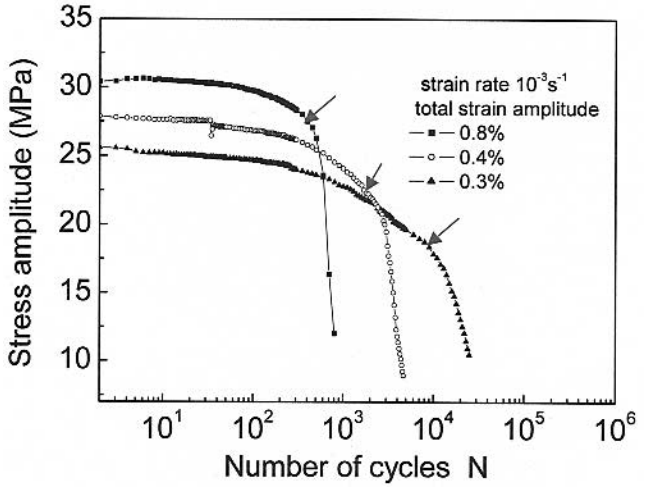

Fig. 2. Cyclic stress history of the Sn-Ag-Cu alloy at a constant strain amplitude.

before a dominant or multiple fatigue cracks develop, which then cause rapid softening of the material over a small number of fatigue cycles.[10] As Fig. 2 indicates, no steady-state response was observed in the Sn-Ag-Cu eutectic alloy. Instead, the cyclic softening continued to intensify over most of the fatigue life of the specimen, following the initial decrease in the cyclic stress amplitude until the final failure of the specimen.

The cycle-dependent softening curves of the Sn-Ag-Cu alloy could be divided into two major stages. In the initial stage, the cyclic stress amplitude decayed gradually with the number of fatigue cycles, and the specimen maintained most of its load-carrying capacity. This was then followed by the final stage where the cyclic stress amplitude fell rapidly. If the sharp turns were used to separate the two stages on the softening curves, the transition from the initial to the final stage, marked by arrows in Fig. 2, would occur when the stress amplitude fell to 75% to 85% of the initial peak.

Stress-Strain Response

For each fatigue cycle, the relationship between stress and strain is strongly dependent on loading history. The dependence is shown in Fig. 3, where the stress-strain curves for successive cycles are given for an applied strain amplitude of 0.8%. Initially, the stress-strain curve of the alloy followed a nearly symmetrical hysteresis loop, typical of most ductile metals. During fatigue cycling, the size of the hysteresis loop decreased with the number of fatigue cycles. After 500 cycles, the hysteresis loops became notably smaller. Such a progressive reduction of the loop size is consistent with the variation of the cyclic stress amplitude with the cycle number shown in Fig. 2.

With continued cycling, the shape of the hysteresis loop also changed significantly. In the initial cycle, the loop contained long, well-defined elastic regions. Those elastic regions could be readily identified as the linear segments on the left and right side of the loop. However, as the cycle number increased, the elastic regions became smaller and smaller until the linear segments were unintelligible in the loop. In addition, the loop turned slightly asymmetric in tension and compression, with the apparent yield strength slightly higher in compression than in tension.

Cyclic Stress-Strain Curves

The cyclic deformation behavior of the Sn-Ag-Cu alloy is shown in Fig. 4 by the plastic region of the cyclic stress-strain curve. The curve at 1/4 cycle represents the monotonic stress-strain response. Because the cyclic stress amplitude did not reach a steady-state level, cyclic stress-strain curves were drawn at fractions of the fatigue life, N_f, which was taken as the number of cycles to which the stress amplitude had fallen to 75% of the initial stress amplitude. For all fractions of the fatigue life, the cyclic stress-strain curve was below the monotonic level, indicating that the solder alloy cyclically softened. In the first half of the fatigue life, cyclic softening was more pronounced at lower strain amplitudes, resulting in a steeper stress-strain curve under cyclic loading than under monotonic loading. However, by the later stage of the life ($75\%N_f$), the cyclic stress-strain curve was nearly parallel to the monotonic one. In both monotonic and cyclic cases, the flow stress varied by less than 20% over the entire range of strains. Such a small rise in the flow stress corresponds to an apparently low work-hardening rate for the alloy, which may be related to offsetting effects of thermally activated softening processes.[11]

If the decrease in the flow stress with fatigue cycle is used as an indicator of the extent of the fatigue damage for a given strain amplitude, Fig. 4 indicates that the accumulation of the fatigue damage in the Sn-Ag-Cu alloy depended on strain amplitude. At low strain amplitudes, the fatigue damage was evenly distributed over the entire life. At high strain amplitudes, however, most of the fatigue damage apparently was introduced in the later stage of life.

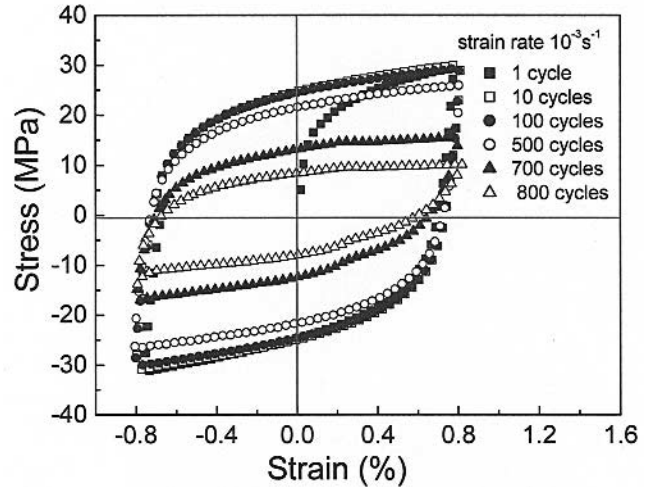

Fig. 3. Hysteresis loops of Sn-Ag-Cu alloys at a strain amplitude of 0.8%.

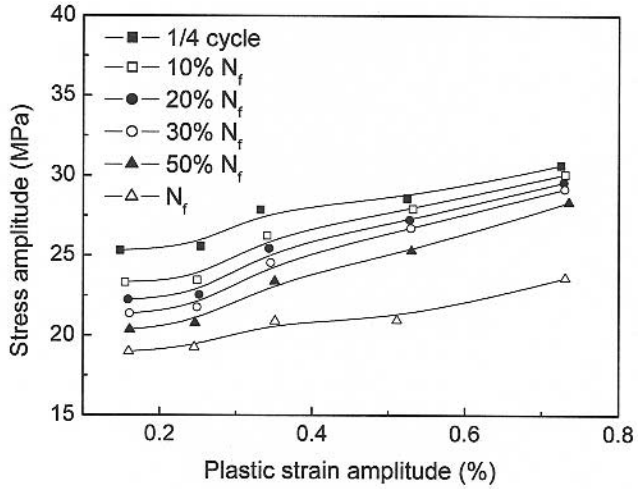

Fig. 4. Cyclic stress-strain curves of the Sn-Ag-Cu alloy.

Microcrack Development

Numerous microcracks were found on the surface of the fatigue specimen at various stages of the fatigue life, as shown in Fig. 5. Most of the microcracks tended to follow the grain boundaries of the Sn-rich phase. They appeared very early in the fatigue life. At 1% strain amplitude, surface cracks were observed as early as 30 cycles, less than 10% of the fatigue life (Fig. 5a). At a strain-amplitude of 0.2%, grain boundary cracking was found at less than 5% of the fatigue life (Fig. 5b). Similar damage was observed previously in high-Pb and Sn-Ag solder alloys.[12,13] At low strain amplitudes, a small percentage of the microcracks were also seen in the grains, along the persistent slip bands (Fig. 5b). For a given strain amplitude, the density of the microcracks increased with fatigue cycle. At the larger strain amplitude of 1%, the crack density at the end of the fatigue life was higher than that for the smaller strain amplitude of 0.2% even though the specimen was cycled for fewer number of cycles.

Many of the intergranular cracks tended to form around the finer grains, 30 μm or smaller (Fig. 5a and b), presumably because of the higher area density of the grain boundary per unit volume. At the triple junction of the grain boundaries, corners of the neighboring grains were mismatched (Fig. 5b). The mismatch indicates that the grain boundary sliding may be involved in development of the microcracks. This apparently agrees with the observation of Kanchnomai et al. that the dominant deformation mechanism in the Sn-Ag-Cu alloy at 10^{-3} sec^{-1} consisted of both the deformation of the matrix and grain boundary sliding.[14]

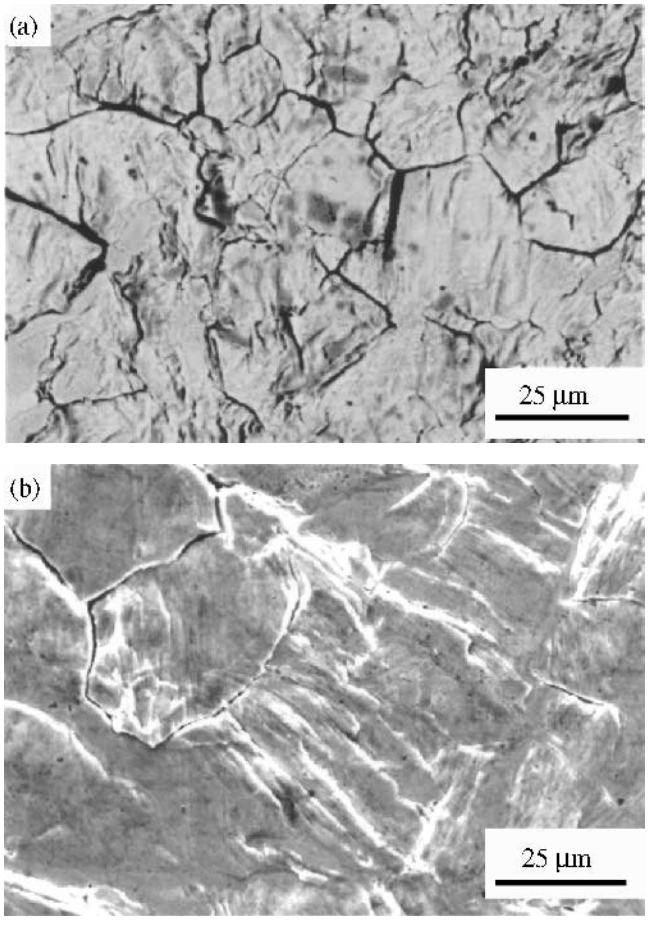

Fig. 5. The SEM images of microcracks on the fatigue specimen surfaces: (a) total strain amplitude 1% and (b) total strain amplitude 0.2%. The loading direction was horizontal.

DISCUSSION

In most metals, the fatigue failure process consists of cyclic deformation, crack initiation, microcrack growth, and macrocrack propagation.[15] The development of microcracks along the slip bands in Fig. 5b indicated that, in the interior of the grain, the Sn-Ag-Cu alloy in this study underwent similar fatigue-damage progression prior to the formation of a macrocrack. However, extensive intergranular cracking shown in Fig. 5 complicated the analysis of fatigue behavior of the Sn-Ag-Cu alloy. These microcracks appeared along isolated grain boundaries early in the fatigue cycle. As fatigue cycle increased, their number grew gradually. It was the linkage of these intergranular microcracks later in the fatigue life that eventually resulted in the final failure of the alloy. In the following, the microcracking analysis based on the approach of Stolkarts et al.[16] is used to show that accumulation of microcracking density with fatigue cycling to the percolation threshold could lead to cycle-dependent softening observed in the eutectic Sn-Ag-Cu alloy.

Consider a polycrystalline alloy cube of length, L, which is made of identical cubic grains, with length, d. Under cyclic loading, some of the individual grain boundaries are cracked, creating a microcracked solid with a microcrack density, ω. As a result of microcracking, the elastic modulus and Poisson's ratio of the solid are reduced to $\bar{E}$ and $\bar{\upsilon}$ from the initial values, E_0 and ν_0:[17]

$$\bar{E} = E_0\left[1-\frac{16\left(1-\bar{\upsilon}^2\right)(10-3\bar{\upsilon})}{45(2-\bar{\upsilon})}\omega\right] \tag{1a}$$

$$\omega = \frac{45\left(\upsilon_0-\bar{\upsilon}\right)(2-\bar{\upsilon})}{16\left(1-\bar{\upsilon}^2\right)\left[10\upsilon_0-\bar{\upsilon}\left(1+3\upsilon_0\right)\right]} \tag{1b}$$

At a constant strain amplitude, the stress amplitude will be reduced to $\bar{\sigma}$ from the initial reading of σ_0. For elastic or perfectly plastic materials, the peak stress should be proportional to the elastic modulus so that

$$\frac{\bar{\sigma}}{\sigma_0} = 1-\frac{16\left(1-\bar{\upsilon}^2\right)(10-3\bar{\upsilon})}{45(2-\bar{\upsilon})}\omega \tag{2}$$

For a given strain amplitude, if the evolution of the microcrack density with fatigue cycle is known, Eq. 2 can be combined with Eq. 1b to calculate the variation of the stress amplitude with fatigue cycle, N. Following the approach of the damage mechanics,[16,18]

the accumulation of the microcrack density with fatigue cycle may be expressed as

$$\omega = A\varepsilon_a^{\chi} N \tag{3}$$

where ε_a is the strain amplitude, N is the number of fatigue cycle, and A and χ are material constants. The terms A and χ can be obtained from experimental measurements by applying the percolation theory.

According to Zallen,[19] the probability, P_c, at which one of the grain boundary edges will be cracked in the simple cubic lattice is equal to 0.247 at the percolation threshold, assuming that the broken grain boundary will open up into nonoverlapping circular cracks. When L >> d, the volumetric density of microcracks at the threshold is equal to $\omega_c = 0.093$ from the geometric analysis. For the eutectic Sn-Ag-Cu alloy, Poisson's ratio should be very close that of pure Sn, which is equal to 0.33.[20] Insertion of ω_c into Eqs. 1b and 2 gives $\bar{\sigma}/\sigma = 0.84$. If such a drop in the stress amplitude is reached at $N = N_f$, the constants A and χ can then be found from

$$\omega_c = A\varepsilon_a^{\chi} N_f \tag{4}$$

by plotting ε_a against N_f, as shown in Fig. 6. Fitting of the experimental data in Fig. 6 to Eq. 4 gives $\chi = 1.724$ and $A = 0.7572$ for the eutectic Sn-Ag-Cu alloy.

Based on the preceding analysis, the cyclic softening of the alloy can be predicted by combining Eqs. 2 and 3:

$$\frac{\bar{\sigma}}{\sigma_0} = 1 - \frac{16\left(1-\bar{\upsilon}^2\right)(10-3\bar{\upsilon})}{45(2-\bar{\upsilon})} A\varepsilon_a^{\chi} N \tag{5}$$

Using the constants A and χ from Fig. 6, the predicted stress amplitudes are given as a function of the cycle number for three strain amplitudes in Fig. 7. In all three cases, the general agreement between the theoretical predictions of Eq. 5 and experimental data is quite good. Therefore, the cycle-dependent cyclic softening behavior observed in the Sn-Ag-Cu alloy stemmed from the accumulation of intergranular microcracks until the microcrack density reached the percolation threshold.

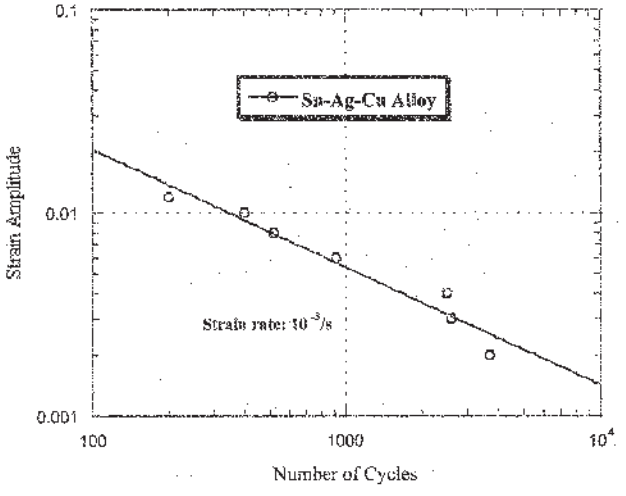

Fig. 6. Strain amplitude, ε_a, versus the number of cycles, N_f, to reach the percolation threshold.

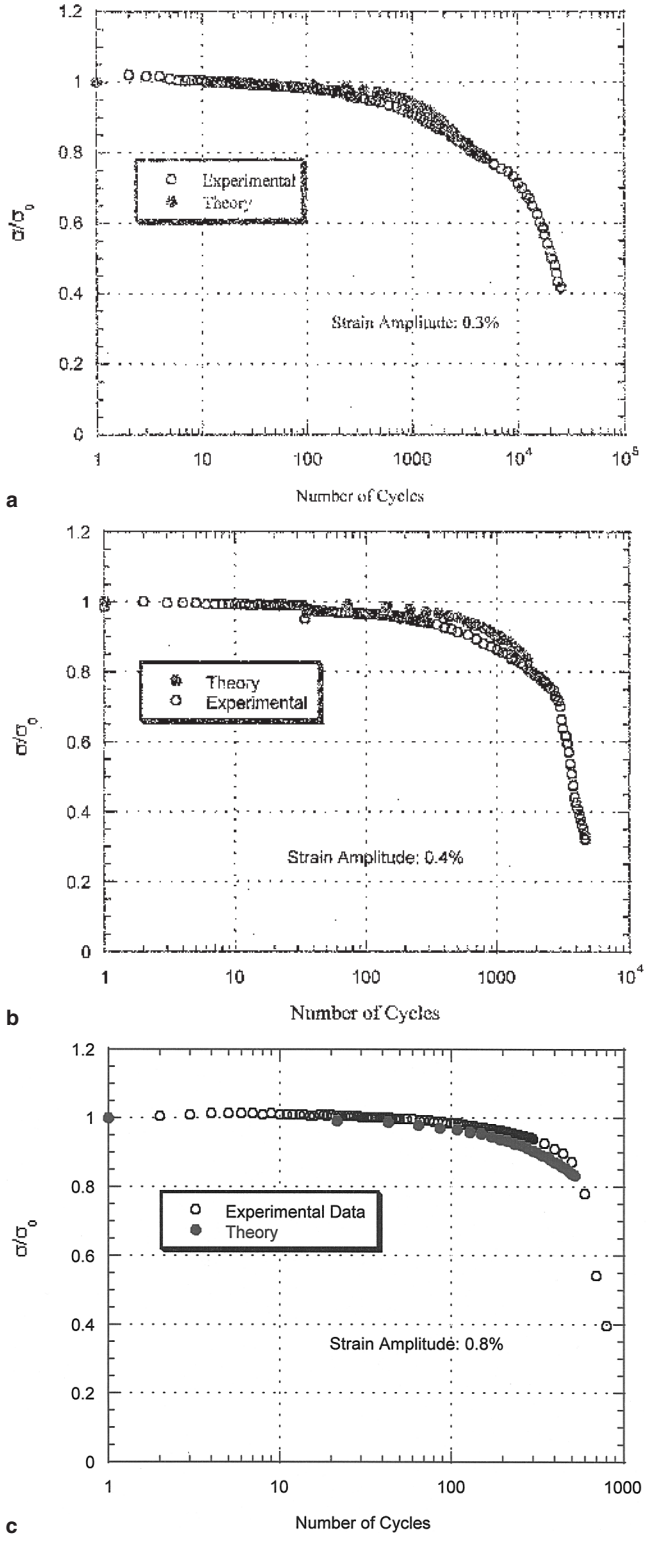

Fig. 7. Comparison of the predicted cyclic-softening behavior with the experimental data at strain amplitudes of (a) 0.3%, (b) 0.4%, and (c) 0.8%.

Beyond the percolation threshold, spontaneous coalescence of the microcracks is expected to lead to

macrocrack formation, which would greatly accelerate the decay of the stress amplitude. As Fig. 7 shows, rapid falls of stress amplitude indeed followed the percolation point. Subsequent deterioration of the alloy is mainly due to propagation of large cracks, which is well characterized by a fracture mechanics approach, based on linear or nonlinear fracture-mechanics driving force, such as stress intensity factor, K, or J-integral. For Sn-based alloys, both K and J have shown satisfactory correlations with macrocrack growth rate, depending on the loading rate, temperature, and alloy composition.[21]

CONCLUSIONS

Cyclic response of the ternary Sn-Ag-Cu solder alloy was studied under strain control. The alloy exhibited a strong cycle-dependent cyclic softening that began early and persisted through most of the fatigue life. Such a cycle-dependent cyclic-softening behavior was shown to result from early development of microcracks, predominantly along the grain boundaries in the equiaxed grain structure. Most of the intergranular cracks tended to initiate in the areas with finer grains, involving grain boundary sliding.

ACKNOWLEDGEMENTS

Support for this work was provided by the Natural Science Foundation of China through Grant No. 50228101.

REFERENCES

1. I. Ohnuma, M. Miyashita, K. Anzai, X.J. Liu, H. Ohtani, R. Kainuma, and K. Ishida, *J. Electron. Mater.* 29, 1137 (2000).
2. K.W. Moon, W. J. Boettinger, U.R. Kattner, F.S. Biancaniello, and C.A. Handwerker, *J. Electron. Mater.* 29, 1122 (2000).
3. I. Shohji, T. Yoshida, T. Takahashi, and S. Hioki, *Mater. Trans.* 43, 1854 (2002).
4. W. Ren, Z. Qian, M. Lu, S. Liu, and D. Shangguan, *J. Electron. Packaging* 121, 271 (1999).
5. K. Suganuma, *Curr. Op. Solid State Mater. Sci.* 5, 55 (2001).
6. J.H. Lau and Y.H. Pao, *Solder Joint Reliability of BGA, CSP, Flip Chip, and Fine Pitch SMT Assemblies* (New York: McGraw-Hill, 1997).
7. S. Choi, K.N. Subramanian, J.P. Lucas, and T. R. Bieler, *J. Electron. Mater.* 29, 1249 (2000).
8. C. Kanchanomai, Y. Miyashita, and Y. Mutoh, *J. Electron. Mater.* 31, 456 (2002).
9. Y. Kariya and M. Otsuka, *J. Electron. Mater.* 27, 1229 (1998).
10. R.W. Hertzberg, *Deformation and Fracture Mechanics of Engineering Materials* (New York: John Wiley & Sons, 1996). pp. 557–566.
11. W.J. Plumtree, C.R. Gagg, and S. Peters *J. Electron. Mater.* 30, 1178 (2001).
12. S. Vaynman, M.E. Fine, and D.A. Jeannotte, *Metall. Trans. A* 19, 1051 (1988).
13. C. Kanchanomai, Y. Miyashita, Y. Mutoh, and S.L. Mannan, *Mater. Sci. Eng. A* 345, 90 (2003).
14. C. Kanchanomai, Y. Miyashita, and Y. Mutoh, *Int. J. Fatigue* 24, 987 (2002).
15. M.E. Fine, *Metall. Trans. A* 11A, 365 (1980).
16. V. Stolkarts, L.M. Keer, and M.E. Fine, *J. Mech. Phys. Solids* 47, 2451 (1999).
17. B. Budiansky and R.J. O'Connel, *Int. J. Solids Struct.* 12, 81 (1976).
18. L.M. Kachanov, *Introduction to Continuum Damage Mechanics* (Boston, MA: Kluwers Academic Publishers, 1986).
19. R. Zallen, *The Physics of Amorphous Solids* (New York: John Wiley & Sons, 1983).
20. W. Koster and H. Franz, *Metall. Rev*. 21, 1 (1961).
21. J. Zhao, Y. Mutoh, Y. Miyashita, and S.L. Mannan, *J. Electron. Mater.* 31, 879 (2002).